Biochemical Pharmacology 163 (2019) 321–334

Contents lists available at ScienceDirect

Biochemical Pharmacology

journal homepage: www.elsevier.com/locate/biochempharm

Cannabinoid derivatives acting as dual PPARγ/CB2 agonists as therapeutic agents for systemic sclerosis

Adela García-Martín[a,1], Martín Garrido-Rodríguez[b,1], Carmen Navarrete[g], Diego Caprioglio[c], Belén Palomares[d,e,f], Jim DeMesa[g], Alain Rollland[g], Giovanni Appendino[c], Eduardo Muñoz[d,e,f,*]

[a] Emerald Health Biotechnology España, Córdoba, Spain
[b] Innohealth Group, Madrid, Spain
[c] Dipartimento di Scienze del Farmaco, Università del Piemonte Orientale, Novara, Italy
[d] Maimonides Biomedical Research Institute of Córdoba, Spain
[e] Departament of Cellular Biology, Physiology and Immunology, University of Córdoba, Spain
[f] Universitary Hospital Reina Sofía, Córdoba, Spain
[g] Emerald Health Pharmaceuticals, San Diego, CA, USA

ARTICLE INFO

Keywords:
Cannabinoids
Systemic fibrosis
Bleomycin
Inflammation
Vasculopathy
Transcriptomic signature

ABSTRACT

The endocannabinoid system (ECS) may play a role in the pathophysiology of systemic sclerosis (SSc). Cannabinoids acting as dual PPARγ/CB_2 agonists, such as VCE-004.8 and Ajulemic acid (AjA), have been shown to alleviate skin fibrosis and inflammation in SSc models. Since both compounds are being tested in humans, we compared their activities in the bleomycin (BLM) SSc model. Specifically, the pharmacotranscriptomic signature of the compounds was determined by RNA-Seq changes in the skin of BLM mice treated orally with AjA or EHP-101, a lipidic formulation of VCE-004.8. While both compounds down-regulated the expression of genes involved in the inflammatory and fibrotic components of the disease and the pharmacotranscriptomic signatures were similar for both compounds in some pathways, we found key differences between the compounds in vasculogenesis. Additionally, we found 28 specific genes with translation potential by comparing with a list of human scleroderma genes. Immunohistochemical analysis revealed that both compounds prevented fibrosis, collagen accumulation and Tenascin C (TNC) expression. The endothelial $CD31^+/CD34^+$ cells and telocytes were reduced in BLM mice and restored only by EHP-101 treatment. Finally, differences were found in plasmatic biomarker analysis; EHP-101, but not AjA, enhanced the expression of some factors related to angiogenesis and vasculogenesis. Altogether the results indicate that dual PPARγ/CB2 agonists qualify as a novel therapeutic approach for the treatment of SSc and other fibrotic diseases. EHP-101 demonstrated unique mechanisms of action related to the pathophysiology of SSc that could be beneficial in the treatment of this complex disease without current therapeutic options.

1. Introduction

Systemic sclerosis (SSc) or scleroderma is an orphan autoimmune multi-organic disease that affect the connective tissue [1]. The pathophysiology of the disease is complex and includes an innate and an adaptive immune response that promotes the production of autoantibodies, microvascular endothelial cell damage and fibroblast dysfunction leading to excessive accumulation of collagen and other elements of the extracellular matrix contributing to fibrosis [2]. Vasculopathy is a consequence of inflammatory and non-inflammatory processes and in post-mortem studies of patients with SSc, hyperplasia of the intima has been observed in large and small arteries in the absence of vasculitis [3–5]. The alteration of vascular permeability and vascular tone are the earliest signs of vascular dysfunction. In addition,

Abbreviations: AjA, Ajulemic acid; Arg-1, Arginase-1; BLM, Bleomycin; CX3CL1, Chemokine (C-X3-C motif) ligand 1; DLL4, Delta-like 4; ECS, Endocannabinoid System; FGF 1, Fibroblast Growth factor 1; FGF 2, Fibroblast growth factor 2; HGF, Hepatocyte growth factor; KGF, Keratinocyte Growth Factor; PDGF-AA, Platelet-derived growth factor; SMA, α-smooth muscle actin; SSc, Systemic Sclerosis; TNC, Tenascin C; VEGF-B, Vascular Endothelial Growth Factor; vW, von Willebrand

* Corresponding author at: Instituto Maimónides de Investigación Biomédica de Córdoba, Universidad de Córdoba, Avda Menéndez Pidal s/n. 14004, Córdoba, Spain.
E-mail address: fi1muble@uco.es (E. Muñoz).

[1] These authors have contributed equally to this work.

https://doi.org/10.1016/j.bcp.2019.02.029
Received 16 January 2019; Accepted 26 February 2019
Available online 27 February 2019
0006-2952/

activation of platelets and enhanced coagulation with reduced fibrinolysis further contribute to vasculopathy in SSc [6].

The endocannabinoid system (ECS) is composed by the G-protein couple receptors CB_1 and CB_2, endocannabinoids such as anandamide and 2-arachidonoyl glycerol, and the enzymes that regulated their synthesis and catabolism. In addition, cannabinoids of different nature also target ionotropic receptors of the TRP family, and nuclear receptors such as PPARα and PPARγ [7,8]. Accumulated evidence suggests that the ECS could play a role in the pathophysiology of SSc [9]. The blocking of CB_1 alleviated early inflammatory stages of SSc, whereas the activation of CB_1 is detrimental in preclinical murine models of SSc [10,11]. In contrast, ligand-induced CB_2 activation protected against fibrosis and inflammation [12,13]. Indeed, the ECS also regulates vascular endothelial function and CB_2 activation can modulate endothelial cell activation and downregulate the expression of cell adhesion molecules such as Intercellular Adhesion Molecule 1 and Vascular Cell Adhesion Molecule 1 [14].

The peroxisome proliferator-activated receptor (PPAR)-γ is a nuclear receptor that plays a key role in the regulation of lipid metabolism and glucose homeostasis. In addition, PPARγ has been recognized to play a key role in inflammatory processes and connective tissue homeostasis [15]. Importantly, loss of PPARγ function in fibroblasts enhances susceptibility to skin fibrosis in mice. Accordingly, fibroblasts isolated from skin biopsies of SSc patients showed reduced PPARγ expression. Conversely, PPARγ agonists have been shown to prevent inflammation, dermal fibrosis and lipoatrophy in preclinical models of SSc [15–17]. Increased levels of TGFβ is the hallmark of fibrotic diseases, and PPARγ agonists have been shown to inhibit the profibrotic response through inhibition of the TGFβ/SMADs signaling pathway at the nuclear level [18]. In addition, PPARγ ligands normalized PPARγ expression levels, attenuating TGFβ-induced fibroblast activation and differentiation [19].

Based on this information, small molecules such as VCE-004.8 and Ajulemic Acid (AjA), which possess dual PPARγ/CB_2 agonistic activities, represent an attractive pharmacological approach for the management of SSc [17,20]. Indeed, AjA (Lenabasum) has shown efficacy in a Phase 2 clinical trial with dcSSc (diffuse cutaneous SSc) patients (clinicaltrial.gov identifier: NCT02465437), while a recent study suggested that AjA ameliorates inflammation through the generation of pro-resolvin lipid mediators in human volunteers [21]. The relative contribution of the CB_2 receptor and/or PPARγ to this activity is still unclear. We have shown previously that in addition to PPARγ and CB_2, VCE-004.8 also affects the Hypoxia Inducible Factor (HIF) pathway and induces the expression of Arginase 1, which regulates the metabolism of arginine and counteracts the proinflammatory acidity of iNOS [20,22]. In addition, EHP-101, a lipidic formulation of VCE-004.8 that has entered Phase I human development (clinicaltrial.gov identifier: NCT03745001), has been shown to prevent skin and lung fibrosis in the BLM model of SSc and downregulate the expression of several key genes associated with fibrosis and inflammation [23].

Since both compounds are being tested in humans, we were interested in identifying similarities and differences in a murine model of SSc and compared the pharmacotranscriptomic signature of both drug candidates. We now report that EHP-101, an oral lipidic formulation of VCE-004.8, prevents skin and lung fibrosis in a BLM-model of SSs, while also demonstrating a different pharmacotranscriptomic signature and a differential effect on endothelial markers as compared to AjA.

2. Material and methods

2.1. Compounds

Ajulemic acid was prepared according to an improved protocol and the purity was 98.1% [24]. EHP-101 is a lipidic formulation of VCE-004.8 [(1′R,6′R)-3-(Benzylamine)-6-hydroxy-3′-methyl-4-pentyl-6′-(prop-1-en-2-yl) [1,1′bi(cyclohexane)]-2′,3,6-triene-2,5-dione)] [23]. The chromatographic purity of VCE-004.8 in EHP-100 was 97.6%.

2.2. Animals and experimental protocols

Six- to eight-week-old female BALB/c mice were purchased from Harlan laboratories (Barcelona, Spain) and housed in our animal facilities (University of Córdoba, Córdoba, Spain) under controlled conditions (12 h light/dark cycle; temperature 20 °C (± 2°C) and 40–50% relative humidity) with free access to standard food and water. All experiments were performed in accordance with European Union guidelines and approved by the Animal Research Ethics Committee of the Córdoba University (2014PI/016).

Bleomycin-induced fibrosis was developed by daily subcutaneous injections of 100 µL bleomycin (20 µg/mL) diluted in phosphate buffered saline (PBS) (Mylan Pharmaceuticals, Barcelona, Spain) into well-defined areas (1 cm^2) of the shaved backs of mice for 6 weeks. During the last 3 weeks, the mice were treated daily by oral gavage with either EHP-101 (20 mg/kg) or AjA (5 mg/kg). EHP-101 is a formulated lipidic solution of VCE-004.8 (30 mg/mL, Corn oil/Maisine® CC (50/50 (v/v) and the same for AjA. After 6 weeks, all animals were sacrificed by cervical dislocation and dissected for tissue processing. Skin and lung samples were divided into two pieces, one maintained in RNA-later (Sigma-Aldrich, St. Louis, MO, USA) cooled in dry ice and stored at −80 °C for transcriptomic analysis, and the second piece fixed in fresh 4% paraformaldehyde (0.1 M, PBS) (AppliChem, Darmstadt, Germany) for histochemical analysis. Six to eight animals were analyzed in each experimental group.

2.3. Histochemical analysis

Five µm-thick tissue sections of skin or lung sections were embedded in paraffin and then stained with Masson's trichrome (Merck Millipore, Darmstadt, Germany). Skin collagen was also detected by picrosirius red staining (Sigma-Aldrich, St. Louis, MO, USA). Three random fields of each skin or lung biopsy were photographed by standard brightfield microscopy and digitalized using a Leica DFC420c camera and analyzed using Image J software (http://rsb.info.nih.gov/ij/) in a blinded manner by two independent observers. The Ashcroft score was used to determine the degree of fibrosis in lung specimens as previously described [25].

2.4. Confocal microscopy analyses

Skin sections (5 µm-thick) were deparaffinized and boiled for 10 min in sodium citrate buffer (10 mM, pH 6.0) (Sigma-Aldrich, St. Louis, MO, USA) for antigen retrieval.

The sections were then incubated in a PBS washing buffer containing 0.1% Triton X-100 and 0.1% Saponin (Sigma-Aldrich, St. Louis, MO, USA) three times for 10 min. Nonspecific binding was blocked with 3% bovine serum albumin (BSA) (Sigma-Aldrich, St. Louis, MO, USA) in PBS and sections were incubated overnight at 4 °C with the following primary antibodies: monoclonal anti-Tenascin (TNC) (1:100 dilution, #MAB2138, RD system, Mineapolis, MN, USA), polyclonal anti-CD31 (1:100 dilution, ab28364, Abcam, Cambridge, UK), rat anti-CD34 (1:100, #553731 BD Biosciences, BD biosciences, San Jose, CA), anti-Von Willebrand (vWF) (1:100, sc-53466, Santa Cruz Biotechnology, Dallas, TX, USA), anti-Arginase-1 (Arg-1) (1:100 dilution, #ab60176, Abcam), and anti-α-Smooth muscle actin (SMA) monoclonal antibody Alexa-488 (1:100 dilution, #53-9760-80, Thermo Fischer, Waltham, MA, USA). After three washes for 10 times each in wash buffer, slides were incubated with secondary antibodies for 1 h at room temperature in the dark. The following secondary antibodies were used in 1:100 dilution: anti-rabbit Texas Red (#A-6399), anti-rat Alexa 488 (#A-11006), anti-mouse Alexa 647 (#A-21235) (Thermo Fischer Scientific, Waltham, MA, USA). The tissue sections were then mounted using Vectashield Antifade Mounting Medium with DAPI (H-1200, Vector

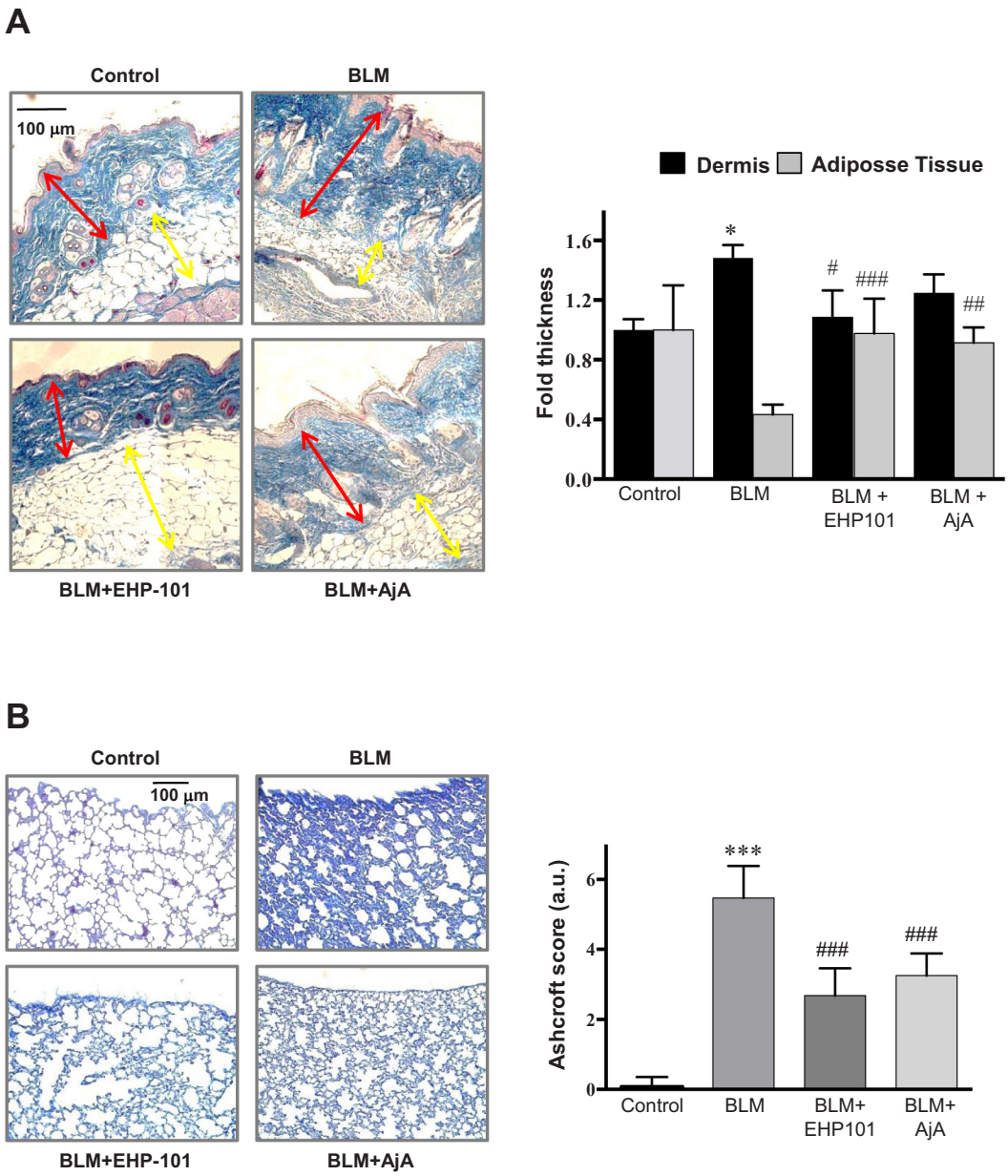

Fig. 1. EHP-101 and AjA prevent skin and lung fibrosis induced by BLM. (A) Images show Masson's trichrome staining (left panel) and their respective quantification of skin from BLM- treated mice (right panel). Red arrows indicate dermal thickness and yellow arrows indicate subcutaneous adipose layer. The statistical analyze has been assessed by parametric One-way ANOVA followed by Bonferroni's post-hoc test. (B) Representative lungs images of Masson's trichrome staining (left panel). Comparison of the Ashcroft score among the experimental groups (right panel). Kruskal-Wallis test followed by Dunn's test for multiple comparisons was used to check for statistical differences between groups. Data are presented as mean ± SEM (n = 8 animals per group), repeated with three independent experiments. Three areas were analyzed of each mouse; *$p < 0.05$, *** $p < 0.001$ versus control group; #$p < 0.05$, ##$p < 0.01$, ###$p < 0.001$ versus BLM group. (For interpretation of the references to color in this figure legend, the reader is referred to the web version of this article.)

Laboratories, Burlingame, Ca, USA) before the slides were washed 3 times for 10 min. All images were acquired using a spectral confocal laser-scanning microscope LSM710, (Zeiss, Jena, Germany) with a 25×/0.8 Plan-Apochromat oil immersion lens and quantified in 10–15 randomly chosen fields using ImageJ software (http://rsb.info.nih.gov/ij/).

2.5. Determination of plasmatic biomarkers

Changes in the relative levels of mouse cytokines, adipokines and angiogenesis-related proteins were determined in plasma using Proteome Profiler Arrays. Plasma from 4 animals from each group were pooled (130 µL) and loaded in the array membranes to detect levels of relevant biomarkers following the manufacturer's protocol (Proteome Profiler™ #ARY028, #ARY015, #ARY013; R&D Systems, Minneapolis, MN, USA). The average signal of the pair of duplicate spots, representing each protein, was calculated after subtraction of background values (pixel density) from negative control spots and normalization to average values from positive control spots using HLImage++ software (Version 22.0.0a; R&D Systems, Minneapolis, MN, USA).

2.6. RNA sequencing

RNA extraction and sequencing were performed for the 6 samples that were not previously sequenced. Total RNA was isolated from frozen mouse skin tissue using QIAzol lysis reagent (Qiagen, Hilden,

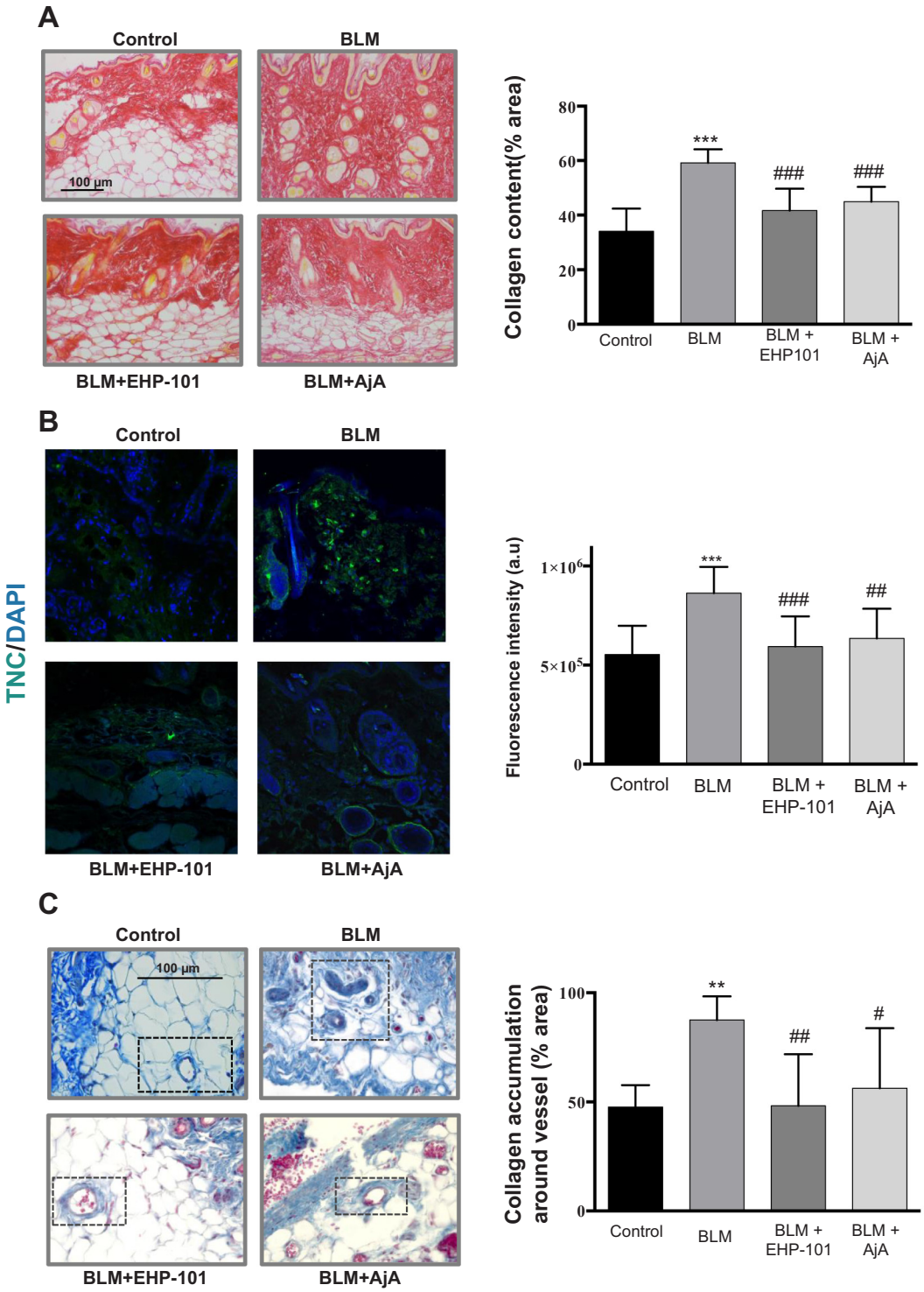

Fig. 2. EHP-101 and AjA reduce collagen content, collagen around blood vessels accumulation and fibrotic markers in skin of BLM mice model. (A) Representative images of collagen staining by picrosirius red dye (left panel) and their quantification (right panel). One-way ANOVA and Bonferroni post-test were used to check for statistical differences between treatment. (B) The immunofluorescence labelling of TNC (green fluorescence) of control, BLM + vehicle, BLM + EHP-101 and BLM + AjA is shown in left panel (original magnification × 25) and their quantification in shown on right panel. Kruskal-Wallis test followed by Dunn's test for multiple comparisons was used to check for statistical differences between groups. (C) Representative images of Masson's trichrome stained skin sections showing collagen associated to blood vessels (indicated with frames) (left panel). Quantification of collagen accumulation (right panel). One-way ANOVA test and for the post-hoc test Bonferroni was used. Data are presented as mean ± SEM (n = 8 animals per group), repeated with three independent experiments. Three areas were analyzed of each mouse; ** $p < 0.01$ ***$p < 0.001$ versus control group; #$p < 0.05$, ##$p < 0.01$, ###$p < 0.001$ versus BLM group. (For interpretation of the references to color in this figure legend, the reader is referred to the web version of this article.)

Germany) and purified with RNeasy mini kit (Qiagen, Hilden, Germany). Transcriptome libraries were constructed with TruSeq Stranded Total RNA LT Sample Prep Kit (with Ribo-Zero Human/Mouse/Rat, #RS-122-2201, Illumina, San Diego, USA). In brief, 300 ng of total RNA from each sample was used to construct a cDNA library, followed by sequencing on the Illumina Hiseq 2500 with single end 50 bp reads and ~30 million reads per sample.

2.7. Bioinformatics and data analysis

Sequencing data for this study (GSE121659) was combined with the data from our previous work (GSE115503) in a unified bioinformatic analysis to achieve three biological replicates for every condition studied. The pre-processing and alignment were performed as previously described [23]. Briefly, sequences were processed with Trimmomatic v0.36 [26], aligned to mouse genome assembly mm10 using HISAT2 v2.1.0 [27] and the counts per gene were obtained with featureCounts v1.6.1 [28]. After this, counts per gene matrices, one for GSE115503 and one for GSE121659, were combined in a single matrix that was analyzed using DESeq2 v1.20.0 [29]. DESeq2 estimates the dispersion and the library size factors from the raw count matrix and applies a negative binomial GLM fitting followed by a Wald test to evaluate the contrasts. Only genes with 15 or more counts across all samples were processed, resulting in a total of 19,436 genes. To control the possible batch effect generated by the different sequencing dates, an additional variable was included in the design formula, indicating whether a sample was sequenced in the first or second assay. The differential expression analysis was performed using the negative binomial linear models included in DESeq2. All genes with an adjusted $p < 0.05$ and an absolute Fold Change > 1.5 were considered as differentially expressed genes. The functional analysis was applied using clusterProfiler v3.8.1 [30]. Gene set enrichment analyses [31] were carried out by ranking the gene lists for each comparison using the log2 transformed Fold Change. The gene sets included in the MSigDB hallmarks collection [32] were analyzed and only those with an adjusted $p < 0.01$ were considered as enriched in any direction. The over representation analyses were performed using the functional categories defined by the Gene Ontology (Biological Process) annotation included in the package org.Mm.eg.db v3.5.0. The whole genome was used as statistical background to assess the over representation of the functional categories in every set of up and down regulated genes. Only terms with a Fisher's Exact Test adjusted $p < 0.01$ were considered as statistically over represented. Regarding the human scleroderma intrinsic genes, the list attached to the GEO entry GSE9285 was downloaded and intersected with the interesting groups of genes from our study. All the intersections including human genes were performed using the HUGO gene symbol nomenclature and the results were graphically represented using the UpSetR v1.3.3 package. All the *p*-values were corrected using the Benjamini & Hochberg adjustment to control the false discovery rate in multiple hypothesis testing.

2.8. Statistical analysis

All the *in vivo* data are expressed as the mean ± SEM. Results were tested for normal distribution using Shapiro-Wilk normality test. In the Figs. 1A, 2A, and 6D, the data were analyzed using one-way ANOVA followed by Bonferroni's post hoc test. When data were not normally distributed (Figs. 1B, 2B, 6C, E, F and 7), significant differences were studied using the Kruskall-Wallis followed by Dunn's post-hoc test using the GraphPad Prism version 6.00 (GraphPad, San Diego, CA, USA). Minimal statistical significance was set at $p < 0.05$. *p* values, n values are indicated in the associated legends for each figure.

3. Results

3.1. EHP-101 and AjA alleviated skin and lung fibrosis

It has been demonstrated by us and others that AjA and EHP-101 have anti-fibrotic and anti-inflammatory activities in the BLM murine model of fibrosis [20,23,33]. To compare both drug candidates, their effectiveness was re-evaluated side-by-side in the same animal model. In BLM-challenged mice, a significant increase in dermal thickness and collagen content was observed, paralleled by a reduction of subcutaneous adipose layer that was replaced by connective tissue. Both EHP-101 (20 mg/kg) and AjA (5 mg/kg) alleviated skin fibrosis, reduced skin thickness and recovered lipoatrophy to a similar extent (Fig. 1A). In addition, BLM-induced lung fibrosis was alleviated by the treatment with either EHP-101 or AjA (Fig. 1B). To further confirm the anti-fibrotic effect of both compounds, the dermal expression of collagen and Tenascin C (TNC) were investigated. Collagen determination was assessed by quantification of picrosirius red staining of skin and TNC expression was investigated by immunostaining. As depicted in Fig. 2A, an increase in collagen accumulation was observed in BLM mice compared to control animals, and treatment with both drug candidates prevented this accumulation. BLM-induced expression of TNC, another marker of fibrosis [34], was also reduced with the treatment of either EHP-101 or AjA (Fig. 2B). BLM has been reported to increase significantly the vascular wall thickness in the dermis of fibrotic mice [35–37]. Accordingly, BLM induced significant collagen deposition around blood vessels that could be prevented by the treatment with both compounds, however EHP-101 was more efficient than AjA in preventing collagen deposition around vessels (Fig. 2C). In summary, our data confirm previous reports demonstrating the anti-fibrotic activity of EHP-101 and AjA [17,20,23].

3.2. Transcriptomic changes in BLM-challenged mice treated with EHP-101 or AjA

To get an initial perspective of the similarities and differences between both drug candidates in BLM-challenged mice, new RNA samples from skin samples were sequenced, and the resulting datasets were combined with data from the previous study [23] in an unified bioinformatic analysis. By doing this, sequencing data for three biological replicates were obtained for each of the following experimental conditions: Control, BLM, treatment with EHP-101 (BLM + EHP-101) and treatment with AjA (BLM + AjA). The differential expression analysis identified a total of 3155, 970 and 564 genes with significant differences in the BLM versus Control, BLM + EHP-101 versus BLM, and BLM + AjA versus BLM comparisons, respectively (Fig. 3A). As depicted in the intersections shown in Fig. 3B, 391 genes that were up or down regulated in BLM mice changed their level significantly in the opposite direction with both treatments. Independently, 431 genes were found to follow the same pattern only with the treatment with EHP-101 while 84 genes did in the case of the AjA treatment. The results for the differential expression analyses for every comparison are provided in the Supplementary file "DESeq results" at the GEO record GSE121659.

To characterize the changes from a biological perspective, we performed different analyses to explore which functional categories followed a common trend with both compounds. The Gene Set Enrichment Analysis (GSEA) used the whole list of genes for every comparison ranked by the log2 transformed fold change to identify enrichments in one of the two extremes of the list for the functional categories defined by the MSigDB hallmark collection. Fig. 4A shows the hallmarks that were enriched ($p < 0.01$) in the BLM versus Control and in at least one of the BLM + EHP-101 versus BLM and BLM + AjA versus BLM list of genes. The analysis revealed that 7 of the 10 hallmarks that were enriched in one direction in BLM-challenged mice followed the opposite trend after treatment with either EHP-101 or AjA. Among them, the

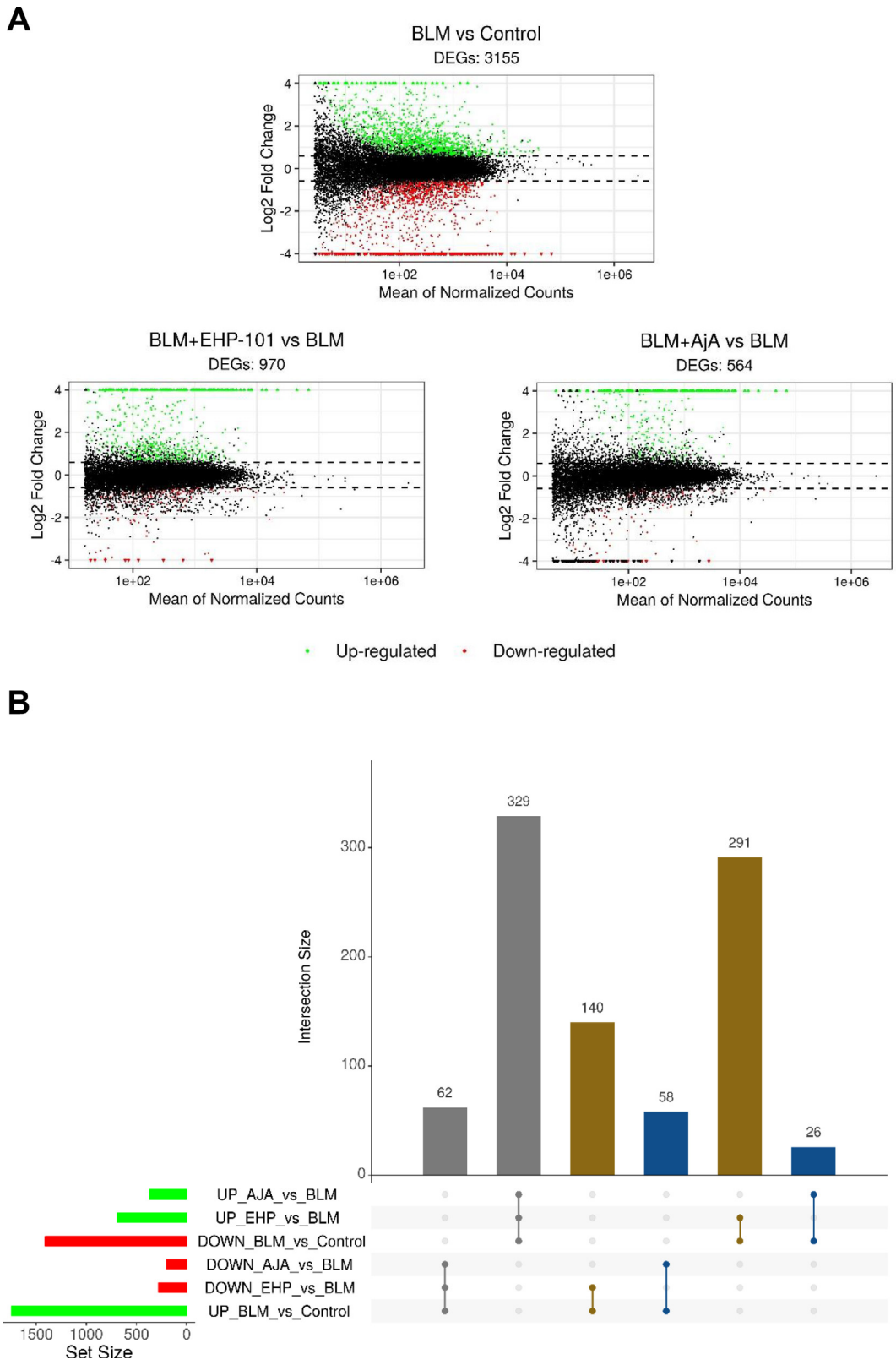

Fig. 3. Differential expression analysis. (A) MA plots indicating the magnitude and significance of the changes for the three comparisons of interest. Red and green points indicate up and down regulated genes, respectively. All genes with an adjusted $p < 0.05$ and an absolute Fold Change > 1.5 for a given comparison were considered as differentially expressed genes (DEGs). (B) Overlapping between the different groups of interesting differentially expressed genes represented as bars over an intersection histogram. The color reflects group of genes that followed the same trend with both treatments, only with the EHP-101 treatment or only with the AjA treatment as grey, yellow and blue, respectively. (For interpretation of the references to color in this figure legend, the reader is referred to the web version of this article.)

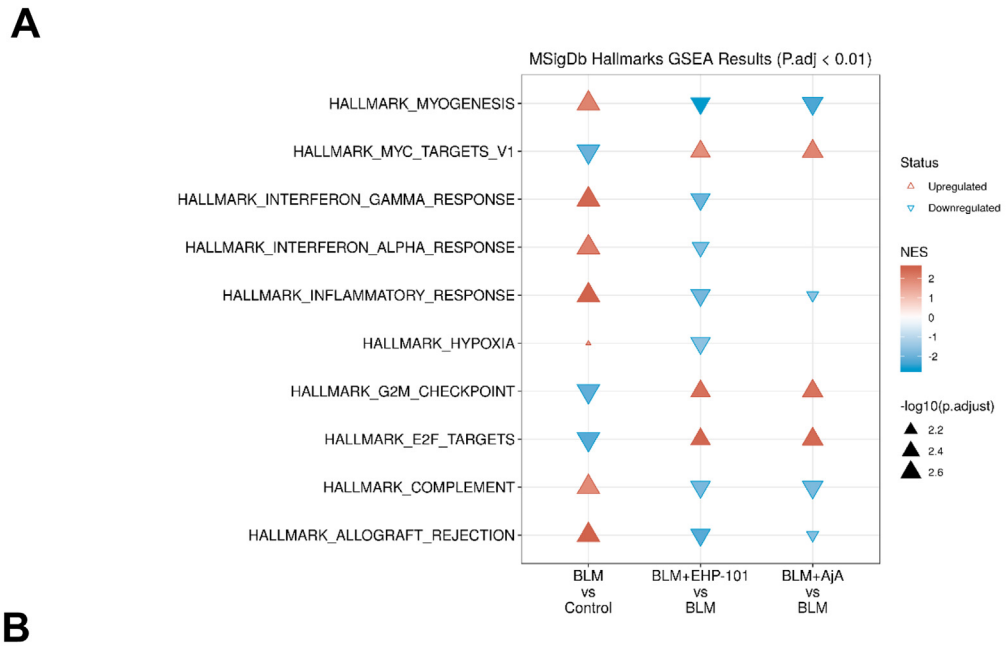

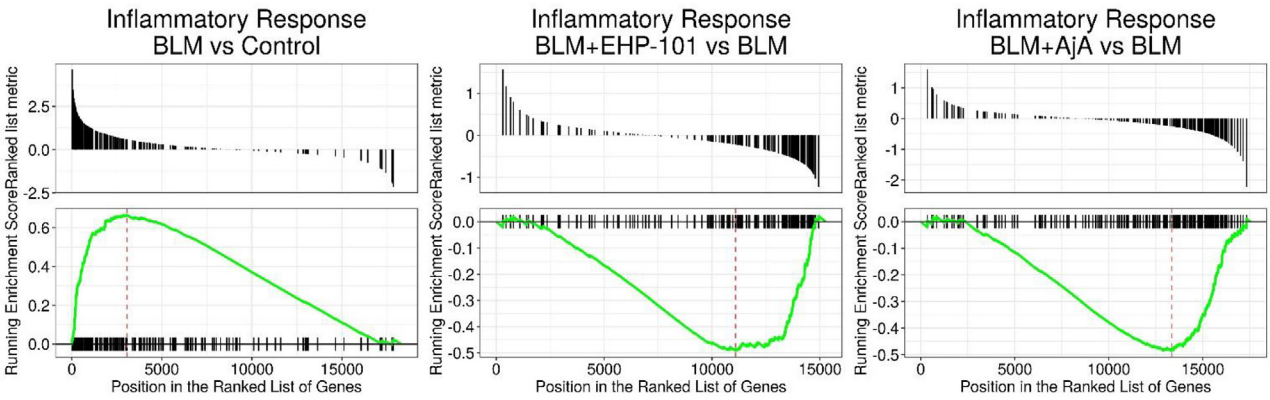

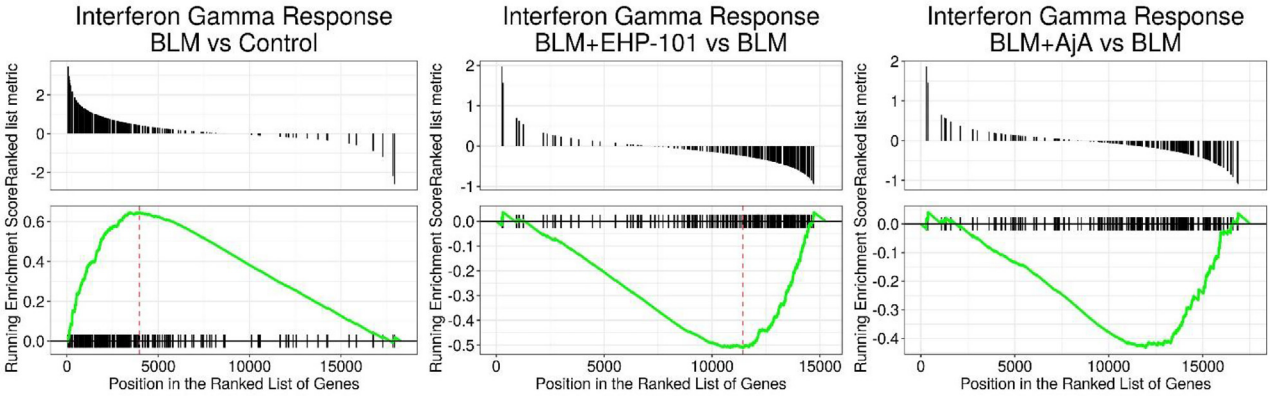

(caption on next page)

Fig. 4. Gene Set Expression Analysis. (A) Hallmarks significantly enriched (adjusted $p < 0.01$) in the BLM vs Control preranked list and in at least one of the other two lists. The direction of the triangles indicates if the enrichment was found in the up or down regulated extreme of the list. The color represents the normalized enrichment score (NES) and the size of the triangles is directly proportional to the significance of the enrichment, as the -log10 transformed adjusted p value. (B), (C) Enrichment plots for the two selected hallmarks in the three lists of genes. The x axis indicates the position of genes in the pre-ranked list among both plots.

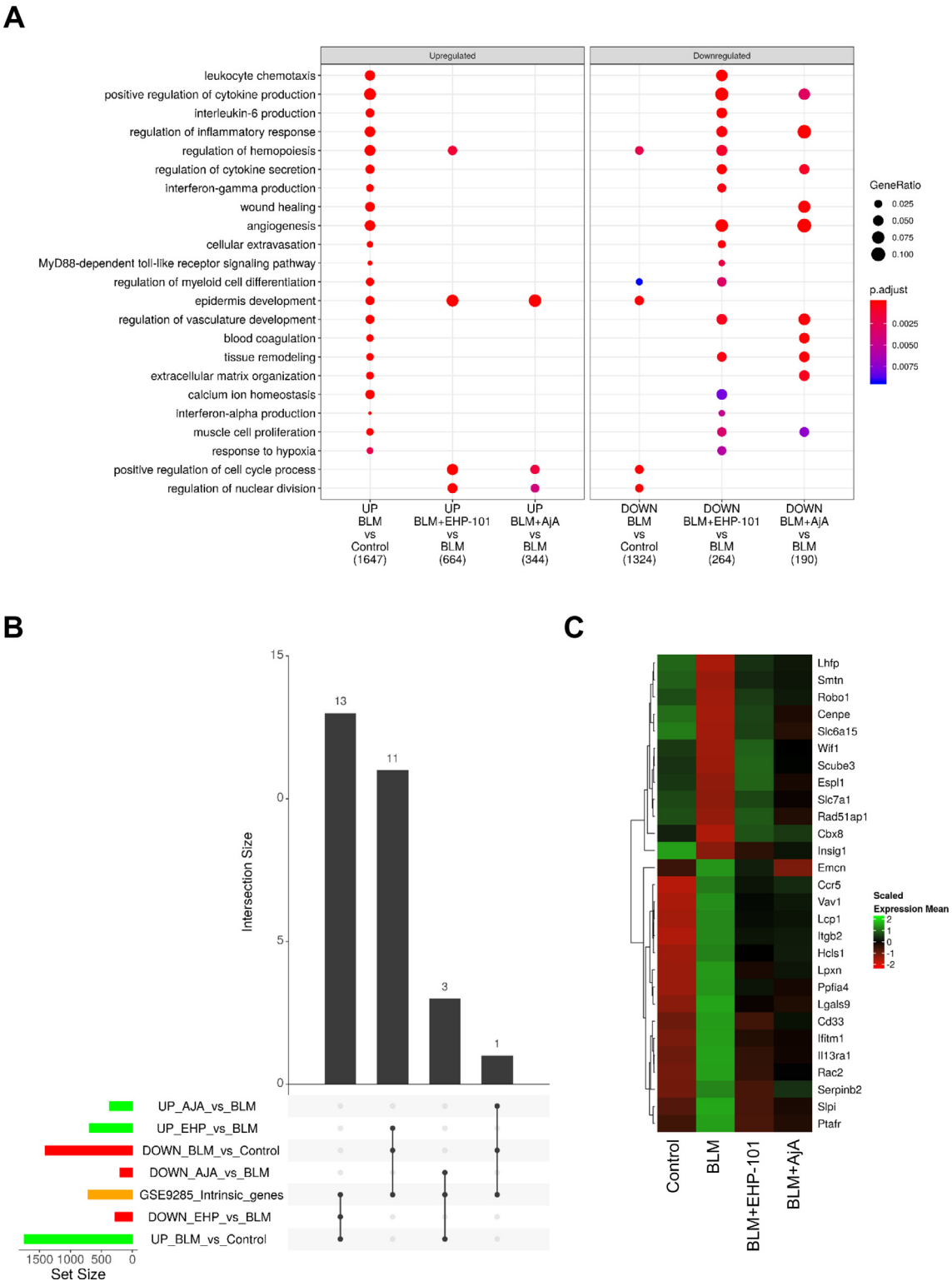

Fig. 5. Overrepresentation analysis and overlap with intrinsic human genes. (A) The dotplot depicts the results of the over representation analysis for selected terms over the different sets of genes. The presence of a point indicates a significant over representation of a term in a group of up or down regulated genes for a given comparison (adjusted $p < 0.01$). (B) Intersection of the treatment-specific genes with the list of intrinsic human scleroderma genes. (C) Heatmap showing the expression levels for the resulting list of 28 genes. Color indicates the mean of scaled regularized log transformed expression values.

inflammatory response and myogenesis hallmarks, related to the pathogenesis of the disease, indicated that both treatments produced a similar effect, which was subsequently confirmed in the histological studies. The three remaining hallmarks that did not follow a common trend consisted of gene sets related to the hypoxia, interferon alpha and interferon gamma response. A significant enrichment for those hallmarks was not found in the comparison of BLM + AjA versus BLM groups. Fig. 4B and C show enrichment plots for a hallmark that followed a common trend with both treatments (inflammatory response) and another that showed a differential response (interferon gamma response).

In a second functional analysis, the different sets of up- and downregulated genes for every comparison were used to perform an over representation analysis, using the gene ontology: biological process annotation as functional categories and the whole genome as statistical background. Fig. 5A shows the selected terms that were overrepresented (Fisher's exact test adjusted $p < 0.01$) in at least two sets of genes. The results of the over representation analysis matched the GSEA results. Some terms such as "regulation of inflammatory response", "positive regulation of cytokine production" or "tissue remodeling" were enriched in the set of genes upregulated in BLM-challenged mice and downregulated by both treatments while others like "response to hypoxia", "interferon-alpha production" and "interferon-gamma production" were enriched only in the downregulated genes by EHP-101. Despite this, the analysis revealed new differential functional categories between both treatments as "wound healing", "blood coagulation" and "extracellular matrix organization" that were enriched in the downregulated genes by AjA. Additionally, some interesting new categories appeared for the EHP-101 treatment as "leukocyte chemotaxis", "MyD88-dependent toll like receptor signaling pathway" or "regulation of hemopoiesis".

Finally, to get some translational insight into our study, genes in which expression increased or decreased significantly with bleomycin and followed the opposite trend with one of the two treatments were compared to a list of "intrinsic" human scleroderma genes obtained from the study carried out by Milano et al. [38]. As shown in Fig. 5B the intersection resulted in a total of 28 genes, with the mean expression for each group plotted and shown as a heatmap (Fig. 5C). Interestingly, genes such are Robo1, Scube3 or Il13ra1 are down- or up-regulated in human SSc and in BLM-mice and normalized more effectively by the treatment with EHP-101.

3.3. EHP-101 prevents vascular damage in BLM-challenged mice

Vascular damage is a key pathogenic factor in SSc from the early stages of the disease [39,40]. Moreover, the presence of $CD31^+/CD34^+$ endothelial cells in capillaries and arterioles is reduced in the dermal cellular network of SSc patients [41]. The observed downregulation of hypoxia-related genes in BLM + EHP-101 mice could reflect a preventive effect of vascular damage related to the fibrotic process induced by BLM. Therefore, we investigated the expression of the endothelial markers CD31 and CD34 and found that BLM-challenged mice showed a reduced expression of these markers reflecting vascular damage (Fig. 6A and C). In addition, the expression of $CD31^+/CD34^+$ cells was used to quantify the number of vessels, which were also reduced in BLM-challenged mice but significantly restored by EHP-101 treatment (Fig. 6E). In contrast, AjA had no effect on preventing vascular damage (Fig. 6E). In addition, EHP-101-treated mice showed an enhanced expression of vWF that may reflect an active angiogenic process [42]. In contrast, the expression of vWF was not modified by AjA treatment in BLM mice (Fig. 6B).

CD34 is also a marker of telocytes that are identified as $CD31^-/CD34^+$ cells. Telocytes are a type of stromal (interstitial) cells whose expression is greatly reduced in fibrotic organs of SSc patients [43,41]. Interestingly, $CD31^-/CD34^+$ expression was significantly reduced in BLM-challenged mice and recovered by EHP-101. The treatment with AjA was not effective to recover the loss of telocytes in BLM mice (Fig. 7A).

3.4. EHP-101 upregulates the expression of Arg-1 in skin

It has already been reported that Arg-1 is considered a marker for macrophage M2 polarization which is important for anti-inflammatory activity [44]. We have previously shown that VCE-004.8 upregulates Arg-1 expression in microglia cells [22]. Furthermore, in the present study, we investigated the effect of EHP-101 on Arg-1 expression in the skin. As shown in Fig. 7B, the expression of Arg-1 was induced by EHP-101 but not by AjA. Therefore, the treatment with EHP-101 could ameliorate BLM-induced inflammation through conversion of arginine to ornithine.

3.5. Effect of EHP-101 and AjA on peripheral biomarkers in BLM-challenged mice

Finally, we determined the impact of both drug candidates on peripheral biomarkers, quantifying the levels of cytokines and other soluble mediators. We found that BLM induction of fibrosis led to an increase in the plasmatic levels of PD-ECGF, PDGF-AA, Proliferin, FGF1, FGF2, VEGF-B, Angiopoietin-3, Endoglin, KGF, Trombospondin-2, and CXC3CL1. Fibrotic mice also showed reduced levels of FGF-21, Serpin E1, HGF and DLL4 (Fig. 8). Some biomarkers such as PD-ECGF, PDGF-AA, Proliferin, FGF basic and acidic, VEGF-B, Angiopoietin-3, Endoglin, KGF, DLL4 and Trombospondin-2 were preferentially or selectively enhanced by EHP-101 treatment. Altogether, these results indicate that EHP-101 and AjA targeted common pathways but that EHP-101 (and not AjA) activated additional pathways that are involved in the angiogenesis and vasculogenesis processes, which have been shown to be important in SSc.

4. Discussion

SSc is a devastating rare disease that currently has no cure. Despite the enormous progress made in understanding the pathophysiology of SSc, the currently available therapies are directed primarily toward the management of organ-specific morbidity [45]. Therefore, novel disease-modifying therapies are urgently needed. Because of the potential to target the ECS at different levels, cannabinoid derivatives have been identified as novel potential anti-fibrotic therapies. We, and others, have previously demonstrated the anti-fibrotic effects of synthetic cannabinoid derivatives in animal models of skin fibrosis [20,23,46–49]. Among them, EHP-101 and AjA (Lenabasum), which are dual $PPAR\gamma/CB_2$ agonists, are two potential drug candidates that have entered clinical development. Since VCE-004.8 (EHP-101) possesses additional properties, such as hypoxia mimetic activity through an effect on the HIF pathway and induction of Arg-1 expression in the skin, we explored the similarities and differences between both drug candidates in a standard murine model of SSc.

To our knowledge, this is the first study that has analyzed the pharmacotranscriptomic differences between these two drug candidates in the skin fibrosis process induced by BLM. Previous transcriptomic analyses have described strong pro-inflammatory and fibrotic upregulated signatures in both SSc mouse models [23,50], and patients [38,51]. Our results reflect that a large group of genes follow a common trend in response to both treatments; in particular, both compounds share a biological signature of down-regulated biological processes, previously shown to be beneficial for the treatment of the disease, such as the regulation of cytokine production [52] or myogenesis, likely resulting from the activation of myofibroblasts [53]. There are several studies that describe the importance of the hypoxia and interferon signaling pathways in systemic sclerosis [54,55] and the absence of a differential inflammatory profile between both compounds led us to question the consequences of other differences in the pathogenesis of

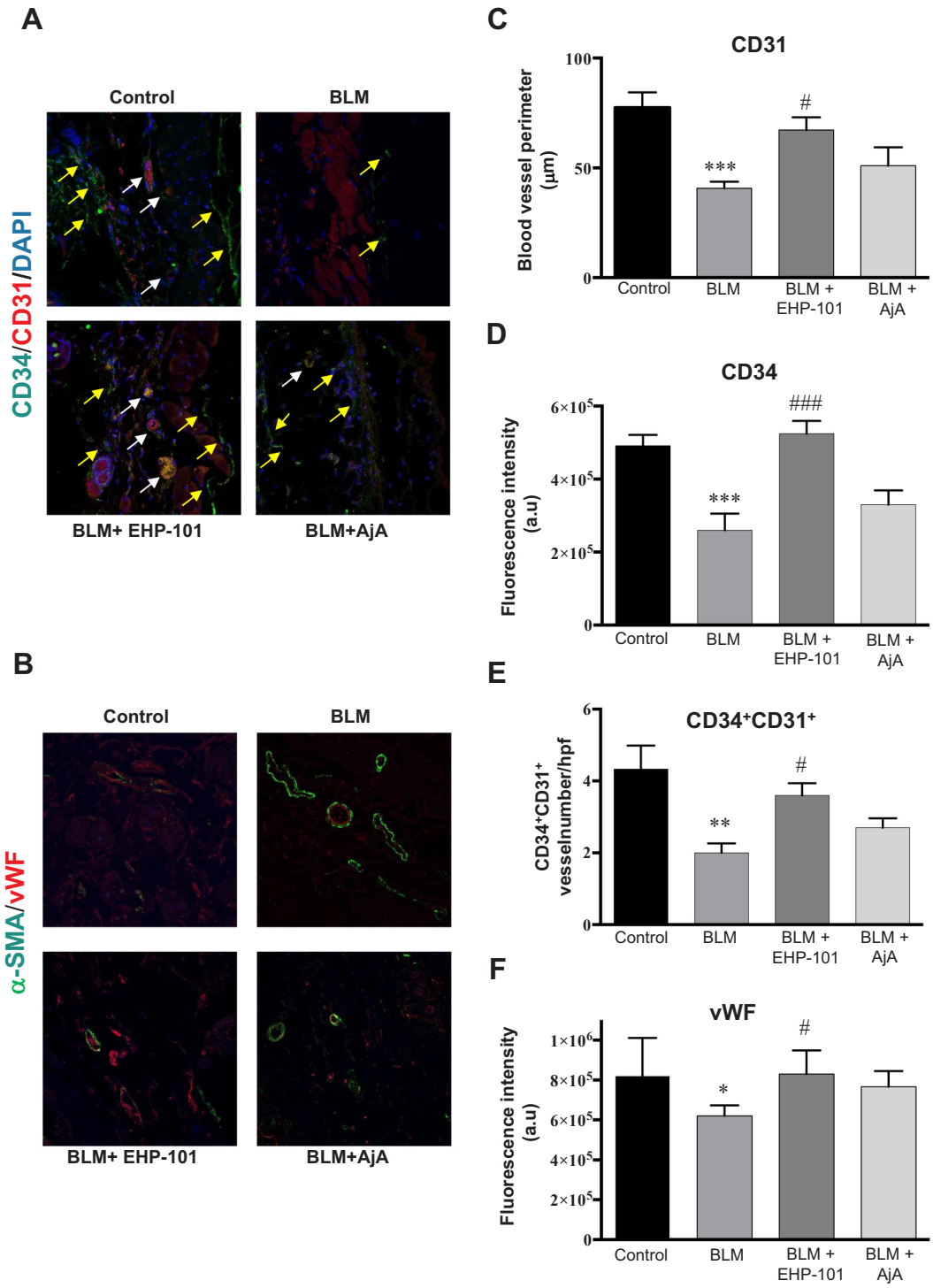

Fig. 6. Effect of EHP-101 and AjA on vascular markers in skin. (A) Double immunofluorescence labelling of skin (CD31, red fluorescence) (CD34, green fluorescence) in control, BLM + vehicle, BLM + EHP-101 and BLM + AjA. CD31 labeling is marker by white arrows and CD34 labeling is marked by yellow arrows. (B) Double immunofluorescence labelling of skin (vWF, red fluorescence) and smooth muscle cells (α-SMA, green fluorescence) in control, BLM + vehicle, BLM + EHP-101 and BLM + AjA. (original magnification × 25). (C) The quantification of $CD31^+$ endothelial cells (average of blood vessel perimeter). Kruskal-Wallis test followed by Dunn's test for multiple comparisons was used to check for statistical differences between groups. (D) The quantification of CD34 expression. The statistical analyze has been assessed by parametric One-way ANOVA followed by Bonferroni's post-hoc test. (E) Number of $CD31^+/CD34^+$ cells. (F) The quantification of vWF expression. Kruskal-Wallis test followed by Dunn's test for multiple comparisons was used to check for statistical differences between groups in figures E and F. Values are expressed as mean ± SEM (n = 8 animals per group), repeated with three independent experiments. Two areas were analyzed of each mouse; $^*p < 0.05$, $^{**}p < 0.01$, $^{***}p < 0.001$, versus control group, $\#p < 0.05$, $\#\#\#p < 0.001$ versus BLM group. (For interpretation of the references to color in this figure legend, the reader is referred to the web version of this article.)

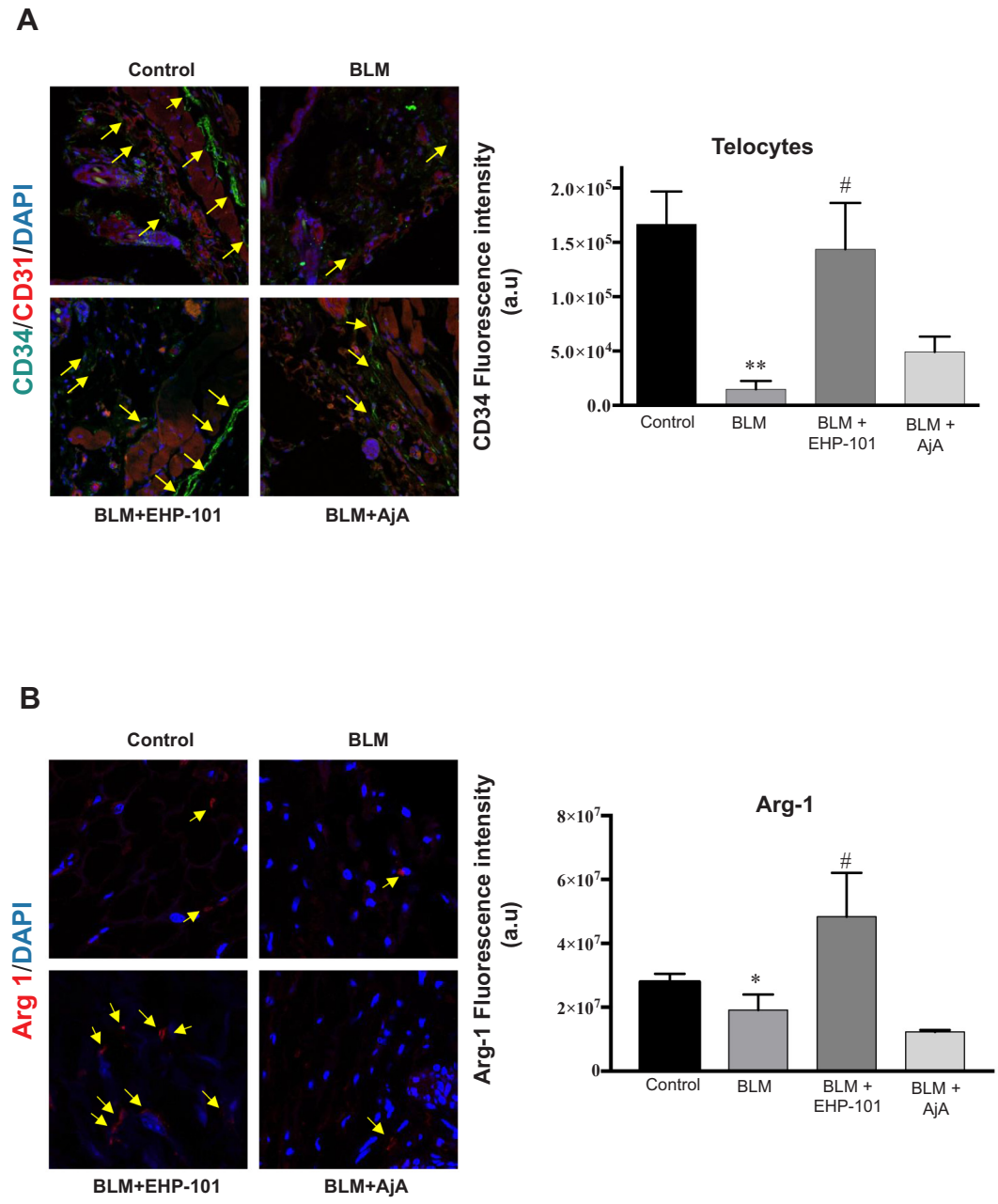

Fig. 7. Effects of cannabinoid drug candidates on telocytes and Arg1 expression. (A) EHP-101 ameliorated BLM-induced loss of telocytes in skin. Double immunofluorescence labelling of skin (CD31, red fluorescence) (CD34, green fluorescence) in control, BLM + vehicle, BLM + EHP-101 and BLM + AjA. Telocytes ($CD34^+/CD31^-$) are marked by yellow arrows (left) and the quantification of CD34 expression in stromal cells, telocytes ($CD34^+/CD31^-$) (right). (B) EHP-101 upregulates the expression of Arg1 in skin. Immunofluorescence labelling of skin (Arg1, red fluorescence) in control, BLM + vehicle, BLM + EHP-101 and BLM + AjA. Arg1 labelling is marked by yellow arrows. Kruskal-Wallis test followed by Dunn's test for multiple comparisons was used to check for statistical differences between groups. Values are expressed as mean ± SEM (n = 8 animals per group), repeated with three independent experiments. Two to three areas were analyzed of each mouse. $*p < 0.05$, $**p < 0.01$ versus control, $\#p < 0.05$ versus BLM group. (For interpretation of the references to color in this figure legend, the reader is referred to the web version of this article.)

SSc.

Despite their common transcriptomic signature, which suggests that both treatments can regulate the inflammatory and fibrotic processes associated with the disease, differences related to other pathways that participate in innate immune system regulation were investigated. Specifically, the interferons (IFNs) and hypoxia signaling pathways are upregulated in BLM mice and appear to be down-regulated by EHP-101, but not by AjA. It has been reported that endothelial cells express type 1 IFN, which is associated with vascular rarefaction in the vessels of SSc patients [56]. In addition, the anti-angiogenic activity of both the IFN-α and IFN-γ may play a role in the vasculopathy associated with SSc [57,58]. Therefore, it is likely that inhibition of these pathways by EHP-101 may account for its ability to protect tissues from vascular damage in BLM-challenged mice. These results are consistent with the ability of EHP-101 to prevent the upregulation of hypoxia-related genes induced by vascular damage. In this sense, the intersection analysis with "intrinsic" human scleroderma genes also showed interesting results. For instance, Robo1 gene expression is downregulated in SSc patients and in BLM mice and such expression is normalized by EHP-101 treatment. Robo (Roundabout) is a family of receptors activated by Slit proteins that are neurovascular guidance molecules. Robo1 and Robo4 are expressed in endothelial cells and the axis Slit2/Robo1 is thought to

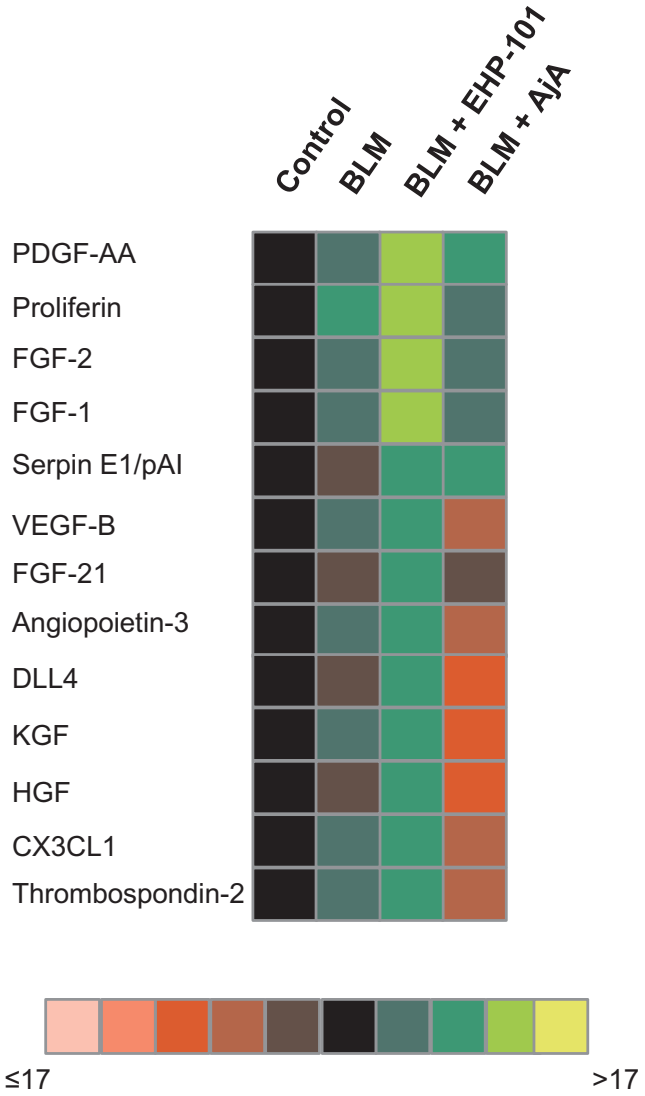

Fig. 8. Comparative plasmatic biomarkers analysis in BLM-challenged mice treated with either EHP101 or AjA. Heatmap showing the proteome profile of cytokines, adipokines and angiogenesis related protein in control, BLM + vehicle, BLM + EHP-101 and BLM + AjA.

mediate endothelial cell migration and angiogenesis. In contrast, the axis Slit2/Robo4 is anti-angiogenic and is upregulated in SSc patients [59]. Whether or not EHP-101 affects the Slit2/Robo4 axis in BLM-challenged mice is an interesting question that remains to be investigated. Scube3 (Signal peptide, CUB and EGF-like domain-containing protein) is another angiogenic factor [60] whose function in SSc pathogenesis has not been investigated. Scube3 expression is also downregulated in the skin of SSc patients and fibrotic mice, and such expression is also normalized by EHP-101 treatment.

Severe tissue hypoxia caused by low cellular oxygen status is thought to play a critical role in the pathogenesis of SSc, even from the early stages of the disease [61]. In this sense, severe hypoxia induced by vascular damage may induce the release of some profibrotic factors that may affect myofibroblast differentiation and fibrosis, increasing vasculopathy [39,62]. However, cellular response to hypoxia is a mechanism of self-defense against low O_2 that seems deficient in SSc, as well as in other hypoxic diseases. Therefore, hypoxia pre-conditioning is an emerging concept that could be also applied to the management of SSc patients. Hypoxia pre-conditioning could mimic the beneficial effects of mild hypoxia by upregulating some protective factors that favor angiogenesis and vasculogenesis. In this sense, HIF-1α and HIF-2α are transcription factors stabilized by hypoxia that regulate the expression of a host of genes whose products are involved in several biological processes, including angiogenesis, vascular tone, and immunity [63].

Our previous results showed that VCE-004.8 also upregulated the expression of Arg-1 in macrophages, which can play a key role in the anti-inflammatory activity of this cannabinoid [22]. Indeed, Arg-1^+ cells were identified in the skin of BLM mice treated with EHP-101 but not in the group of BLM animals treated with AjA (Fig. 7B). Arg-1 is an enzyme that participates in the metabolism of arginine and counteracts the induction of NO by inducible nitric oxide synthase (iNOS). Importantly, it has been detected that iNOS staining increased with the grade of skin lesions in SSc patients, a pattern that parallels endothelial nitrotyrosine expression and vascular damage [64]. On the other hand, arginine consumption by Arg-1, rather than iNOS, represents a well-known immunoregulatory mechanism exploited by anti-inflammatory M2 macrophages, as well as myeloid-derived suppressor cells [65]. It has been also shown that macrophages expressing Arg-1 can suppress Th2-dependent fibrosis [66]. Moreover, Arg-1 expression is crucial for the induction of tolerogenic dendritic cells and, therefore, it is possible that the immunomodulatory activities of EHP-101 could also be of benefit in the management of SSc, as well as other autoimmune diseases such as multiple sclerosis [22]. Experiments are in process to explore whether or not EHP-101 is able to induce an immunosuppressive phenotype in dendritic cells.

To further investigate the effects of EHP-101 on endothelial cells, we performed IHC experiments and found that EHP-101, but not AjA, increased the expression of $CD34^{+/}CD31^+$ cells and recovered the blood vessel perimeters that were reduced in BLM mice. $CD34^{+/}CD31^+$ cells play a significant role in neovascularization [67,68]. Indeed, $CD34^+$ cells isolated from peripheral blood have been used in experimental neovascularization therapies [69]. In addition, we have found that EHP-101, but not AjA, increased the expression of vWF in the endothelium. Some authors have confirmed that this factor may be a marker of disease activity in SSc [70]. Conversely, another publication has suggested that circulating endothelial precursors differentiating into endothelial cells expressing vWF were significantly lower in SSc patients than in healthy controls [71]. Besides, it is well known that reendothelialization of denuded injured vessels must occur rapidly, and this process is essential to avoid complications in patients with SSc. After vascular damage, some growth factors are formed, and adherent activated platelets are recruited to support vascularization. The vWF factor, along with platelets, are attracted to the injury to block the bleeding. Moreover, genetic loss of vWF results in abnormal angiogenesis and angiodysplasia [42]. Altogether, our results suggest that EHP-101 could provide an additional and novel mechanism to improve vasculogenesis and angiogenesis in SSc.

Finally, although the plasma biomarkers studies were performed in a pool of plasma from four mice the proangiogenic effect of EHP-101 was also suggested by some of the biomarkers analyzed in the plasma of BLM mice. Proangiogenic factors such PDGF-AA, Proliferin, KFG and FGF basic and acidic, and VEGF-B were preferentially or selectively enhanced by EHP-101 treatment. These proangiogenic factors can also activate fibroblasts, but the PPARγ agonistic activity of EHP-101 may prevent this profibrotic activity. In support of this assumption we have previously shown that the efficacy of VCE-004.8 on SSc is partially reverted in the presence of a PPARγ antagonist [20]. The selective effect of EHP-101 vs AjA on the plasmatic levels of FGF-21, HGF and DLL4 is also interesting and deserves further research in the context of SSc. To the best of our knowledge the role of FGF-21 in the context of SSc has not been investigated, however FGF-21 has shown antifibrotic activity in fibrotic experimental models [72,73]. DLL4 (delta-like 4) is a Notch ligand expressed in endothelial cells that plays a role in angiogenesis [74]. Interestingly, similar to the results shown in this study, DLL4 expression was also downregulated in BLM-induced pulmonary fibrosis [75] and it is possible that the enhanced levels of this Notch ligand may contribute to the proangiogenic effects of EHP-101. Hepatocyte growth

factor (HGF) may also have therapeutic value in the treatment of SSc because of its ability to inhibit the expression of connective tissue growth factor and collagen deposition in lung fibroblasts from SSc patients [76]. Moreover, HGF is also a proangiogenic factor that may favor productive angiogenesis and vasculogenesis in peripheral diseases [77].

In summary, SSc is a very complex disease, which will be difficult to manage with mono-targeted drugs. Cannabinoids are pleiotropic by nature; therefore, novel synthetic cannabinoids have been developed with the aim to act as disease-modifying drugs. VCE-004.8 (EHP-101) is such an orally available cannabidiol derivative endowed with multi-target activity that shows potential as a novel therapy for the treatment of SSc.

Declaration of interest

EM is a member of the Scientific Advisory Boards of Emerald Health Pharmaceuticals and InnoHealth. AGM is an employee of Emerald Health Biotechnology; Carmen Navarrete, Jim DeMesa and Alain Rolland are employees of Emerald Health Pharmaceuticals.

CRediT authorship contribution statement

Adela García-Martín: Conceptualization, Data curation, Formal analysis, Investigation, Methodology, Writing - original draft. **Martín Garrido-Rodríguez:** Formal analysis, Investigation. **Carmen Navarrete:** Data curation, Investigation. **Diego Caprioglio:** Methodology. **Belén Palomares:** Data curation, Investigation, Methodology. **Jim DeMesa:** Conceptualization, Writing - review & editing. **Alain Rollland:** Conceptualization, Writing - review & editing. **Giovanni Appendino:** Methodology, Writing - review & editing. **Eduardo Muñoz:** Conceptualization, Supervision, Writing - original draft, Writing - review & editing.

Acknowledgements

This work was partially supported by grant SAF2017-87701-R to EM from the Ministry of the Economy and Competition (MINECO), co-financed with the European Union FEDER funds. This work was also partially supported by Emerald Health Pharmaceuticals (San Diego, USA). BP is a predoctoral fellow supported by the iPFIS program, Instituto de Salud Carlos III (IFI15/00022; European Social Fund “investing in your future”).

References

[1] P. Fuschiotti, Current perspectives on the immunopathogenesis of systemic sclerosis, Immunotargets Ther. 5 (2016) 21–35, https://doi.org/10.2147/ITT.S82037.
[2] D. Pattanaik, M. Brown, B.C. Postlethwaite, A.E. Postlethwaite, Pathogenesis of Systemic Sclerosis, Front. Immunol. 6 (2015) 272, https://doi.org/10.3389/fimmu.2015.00272.
[3] W.A. D'Angelo, J.F. Fries, A.T. Masi, L.E. Shulman, Pathologic observations in systemic sclerosis (scleroderma) A study of fifty-eight autopsy cases and fifty-eight matched controls, Am. J. Med. 46 (3) (1969) 428–440.
[4] C.D. Cool, D. Kennedy, N.F. Voelkel, R.M. Tuder, Pathogenesis and evolution of plexiform lesions in pulmonary hypertension associated with scleroderma and human immunodeficiency virus infection, Hum. Pathol. 28 (4) (1997) 434–442.
[5] Y. Nagai, M. Yamanaka, C. Hashimoto, A. Nakano, A. Hasegawa, Y. Tanaka, et al., Autopsy case of systemic sclerosis with severe pulmonary hypertension, J. Dermatol. 34 (11) (2007) 769–772, https://doi.org/10.1111/j.1346-8138.2007.00381.x.
[6] M.M. Cerinic, G. Valentini, G.G. Sorano, S. D'Angelo, G. Cuomo, L. Fenu, et al., Blood coagulation, fibrinolysis, and markers of endothelial dysfunction in systemic sclerosis, Semin. Arthritis Rheum. 32 (5) (2003) 285–295, https://doi.org/10.1053/sarh.2002.50011.
[7] N. Barrie, N. Manolios, The endocannabinoid system in pain and inflammation: its relevance to rheumatic disease, Eur. J. Rheumatol. 4 (3) (2017) 210–218, https://doi.org/10.5152/eurjrheum.2017.17025.
[8] M. Pistis, S.E. O'Sullivan, The role of nuclear hormone receptors in cannabinoid function, Adv. Pharmacol. 80 (2017) 291–328, https://doi.org/10.1016/bs.apha.2017.03.008.
[9] C.D. Rio, E. Millan, V. Garcia, G. Appendino, J. DeMesa, E. Munoz, The endocannabinoid system of the skin. A potential approach for the treatment of skin disorders, Biochem. Pharmacol. (2018), https://doi.org/10.1016/j.bcp.2018.08.022.
[10] K. Palumbo-Zerr, A. Horn, A. Distler, P. Zerr, C. Dees, C. Beyer, et al., Inactivation of fatty acid amide hydrolase exacerbates experimental fibrosis by enhanced endocannabinoid-mediated activation of CB1, Ann. Rheum. Dis. 71 (12) (2012) 2051–2054, https://doi.org/10.1136/annrheumdis-2012-201823.
[11] S. Marquart, P. Zerr, A. Akhmetshina, K. Palumbo, N. Reich, M. Tomcik, et al., Inactivation of the cannabinoid receptor CB1 prevents leukocyte infiltration and experimental fibrosis, Arthritis Rheumatism 62 (11) (2010) 3467–3476, https://doi.org/10.1002/art.27642.
[12] A. Servettaz, N. Kavian, C. Nicco, V. Deveaux, C. Chereau, A. Wang, et al., Targeting the cannabinoid pathway limits the development of fibrosis and autoimmunity in a mouse model of systemic sclerosis, Am. J. Pathol. 177 (1) (2010) 187–196, https://doi.org/10.2353/ajpath.2010.090763.
[13] A. Akhmetshina, C. Dees, N. Busch, J. Beer, K. Sarter, J. Zwerina, et al., The cannabinoid receptor CB2 exerts antifibrotic effects in experimental dermal fibrosis, Arthritis Rheumatism 60 (4) (2009) 1129–1136, https://doi.org/10.1002/art.24395.
[14] Y. Zhao, Z. Yuan, Y. Liu, J. Xue, Y. Tian, W. Liu, et al., Activation of cannabinoid CB2 receptor ameliorates atherosclerosis associated with suppression of adhesion molecules, J. Cardiovasc. Pharmacol. 55 (3) (2010) 292–298, https://doi.org/10.1097/FJC.0b013e3181d2644d.
[15] J. Wei, S. Bhattacharyya, J. Varga, Peroxisome proliferator-activated receptor gamma: innate protection from excessive fibrogenesis and potential therapeutic target in systemic sclerosis, Curr. Opin. Rheumatol. 22 (6) (2010) 671–676, https://doi.org/10.1097/BOR.0b013e32833de1a7.
[16] M. Wu, D.S. Melichian, E. Chang, M. Warner-Blankenship, A.K. Ghosh, J. Varga, Rosiglitazone abrogates bleomycin-induced scleroderma and blocks profibrotic responses through peroxisome proliferator-activated receptor-gamma, Am. J. Pathol. 174 (2) (2009) 519–533, https://doi.org/10.2353/ajpath.2009.080574.
[17] E.G. Gonzalez, E. Selvi, E. Balistreri, A. Akhmetshina, K. Palumbo, S. Lorenzini, et al., Synthetic cannabinoid ajulemic acid exerts potent antifibrotic effects in experimental models of systemic sclerosis, Ann. Rheum. Dis. 71 (9) (2012) 1545–1551, https://doi.org/10.1136/annrheumdis-2011-200314.
[18] A.K. Ghosh, S. Bhattacharyya, J. Wei, S. Kim, Y. Barak, Y. Mori, et al., Peroxisome proliferator-activated receptor-gamma abrogates Smad-dependent collagen stimulation by targeting the p300 transcriptional coactivator, FASEB J. 23 (9) (2009) 2968–2977, https://doi.org/10.1096/fj.08-128736.
[19] A.T. Dantas, M.C. Pereira, M.J. de Melo Rego, L.F. da Rocha Jr., R. Pitta Ida, C.D. Marques, et al., The role of PPAR gamma in systemic sclerosis, PPAR Res. (2015) 124624, https://doi.org/10.1155/2015/124624.
[20] C. del Río, C. Navarrete, J.A. Collado, M.L. Bellido, M. Gómez-Cañas, M.R. Pazos, et al., The cannabinoid quinol VCE-004.8 alleviates bleomycin-induced scleroderma and exerts potent antifibrotic effects through peroxisome proliferator-activated receptor-γ and CB2 pathways, Sci. Rep. 6 (2016) 21703 http://www.nature.com/articles/srep21703#supplementary-informationhttps://doi.org/10.1038/srep21703.
[21] M.P. Motwani, F. Bennett, P.C. Norris, A.A. Maini, M.J. George, J. Newson, et al., Potent anti-inflammatory and pro-resolving effects of anabasum in a human model of self-resolving acute inflammation, Clin. Pharmacol. Ther. (2017), https://doi.org/10.1002/cpt.980.
[22] C. Navarrete, F. Carrillo-Salinas, B. Palomares, M. Mecha, C. Jimenez-Jimenez, L. Mestre, et al., Hypoxia mimetic activity of VCE-004.8, a cannabidiol quinone derivative: implications for multiple sclerosis therapy, J. Neuroinflamm. 15 (1) (2018) 64, https://doi.org/10.1186/s12974-018-1103-y.
[23] A. Garcia-Martin, M. Garrido-Rodriguez, C. Navarrete, C. Del Rio, M.L. Bellido, G. Appendino, et al., EHP-101, an oral formulation of the cannabidiol aminoquinone VCE-004.8, alleviates bleomycin-induced skin and lung fibrosis, Biochem. Pharmacol. (2018), https://doi.org/10.1016/j.bcp.2018.07.047.
[24] M.A. Tepper, R.B. Zurier, S.H. Burstein, Ultrapure ajulemic acid has improved CB2 selectivity with reduced CB1 activity, Bioorg. Med. Chem. 22 (13) (2014) 3245–3251, https://doi.org/10.1016/j.bmc.2014.04.062.
[25] T. Ashcroft, J.M. Simpson, V. Timbrell, Simple method of estimating severity of pulmonary fibrosis on a numerical scale, J. Clin. Pathol. 41 (4) (1988) 467–470.
[26] A.M. Bolger, M. Lohse, B. Usadel, Trimmomatic: a flexible trimmer for Illumina sequence data, Bioinformatics 30 (15) (2014) 2114–2120, https://doi.org/10.1093/bioinformatics/btu170.
[27] D. Kim, B. Langmead, S.L. Salzberg, HISAT: a fast spliced aligner with low memory requirements, Nat. Methods 12 (4) (2015) 357–360, https://doi.org/10.1038/nmeth.3317.
[28] Y. Liao, G.K. Smyth, W. Shi, Feature counts: an efficient general purpose program for assigning sequence reads to genomic features, Bioinformatics 30 (7) (2014) 923–930, https://doi.org/10.1093/bioinformatics/btt656.
[29] M.I. Love, W. Huber, S. Anders, Moderated estimation of fold change and dispersion for RNA-seq data with DESeq2, Genome Biol. 15 (12) (2014) 550, https://doi.org/10.1186/s13059-014-0550-8.
[30] G. Yu, L.G. Wang, Y. Han, Q.Y. He, clusterProfiler: an R package for comparing biological themes among gene clusters, OMICS 16 (5) (2012) 284–287, https://doi.org/10.1089/omi.2011.0118.
[31] A. Subramanian, P. Tamayo, V.K. Mootha, S. Mukherjee, B.L. Ebert, M.A. Gillette, et al., Gene set enrichment analysis: a knowledge-based approach for interpreting genome-wide expression profiles, Proc. Natl. Acad. Sci. U.S.A. 102 (43) (2005) 15545–15550, https://doi.org/10.1073/pnas.0506580102.

[32] A. Liberzon, C. Birger, H. Thorvaldsdottir, M. Ghandi, J.P. Mesirov, P. Tamayo, The molecular signatures database (MSigDB) hallmark gene set collection, Cell Syst. 1 (6) (2015) 417–425, https://doi.org/10.1016/j.cels.2015.12.004.

[33] M. Lucattelli, S. Fineschi, E. Selvi, E. Garcia Gonzalez, B. Bartalesi, G. De Cunto, et al., Ajulemic acid exerts potent anti-fibrotic effect during the fibrogenic phase of bleomycin lung, Respir. Res. 17 (1) (2016) 49, https://doi.org/10.1186/s12931-016-0373-0.

[34] D. Ummarino, Systemic sclerosis: tenascin C perpetuates tissue fibrosis, Nat. Rev. Rheumatol. 12 (7) (2016) 375, https://doi.org/10.1038/nrrheum.2016.99.

[35] T. Yamamoto, S. Takagawa, I. Katayama, K. Yamazaki, Y. Hamazaki, H. Shinkai, et al., Animal model of sclerotic skin. I: local injections of bleomycin induce sclerotic skin mimicking scleroderma, J. Investig. Dermatol. 112 (4) (1999) 456–462, https://doi.org/10.1046/j.1523-1747.1999.00528.x.

[36] T. Yamamoto, Y. Takahashi, S. Takagawa, I. Katayama, K. Nishioka, Animal model of sclerotic skin. II. Bleomycin induced scleroderma in genetically mast cell deficient WBB6F1-W/W(V) mice, J. Rheumatol. 26 (12) (1999) 2628–2634.

[37] T. Yamamoto, I. Katayama, Vascular changes in bleomycin-induced scleroderma, Int. J. Rheumatol. 2011 (2011) 270938, , https://doi.org/10.1155/2011/270938.

[38] A. Milano, S.A. Pendergrass, J.L. Sargent, L.K. George, T.H. McCalmont, M.K. Connolly, et al., Molecular subsets in the gene expression signatures of scleroderma skin, PLoS ONE 3 (7) (2008) e2696, , https://doi.org/10.1371/journal.pone.0002696.

[39] J. Varga, D. Abraham, Systemic sclerosis: a prototypic multisystem fibrotic disorder, J. Clin. Investig. 117 (3) (2007) 557–567, https://doi.org/10.1172/JCI31139.

[40] M. Matucci-Cerinic, B. Kahaleh, F.M. Wigley, Review: evidence that systemic sclerosis is a vascular disease, Arthritis Rheumatism 65 (8) (2013) 1953–1962, https://doi.org/10.1002/art.37988.

[41] M. Manetti, S. Guiducci, M. Ruffo, I. Rosa, M.S. Faussone-Pellegrini, M. Matucci-Cerinic, et al., Evidence for progressive reduction and loss of telocytes in the dermal cellular network of systemic sclerosis, J. Cell Mol. Med. 17 (4) (2013) 482–496, https://doi.org/10.1111/jcmm.12028.

[42] A.M. Randi, K.E. Smith, G. Castaman, von Willebrand factor regulation of blood vessel formation, Blood 132 (2) (2018) 132–140, https://doi.org/10.1182/blood-2018-01-769018.

[43] M. Manetti, I. Rosa, L. Messerini, S. Guiducci, M. Matucci-Cerinic, L. Ibba-Manneschi, A loss of telocytes accompanies fibrosis of multiple organs in systemic sclerosis, J. Cell Mol. Med. 18 (2) (2014) 253–262, https://doi.org/10.1111/jcmm.12228.

[44] N. Takeda, E.L. O'Dea, A. Doedens, J.W. Kim, A. Weidemann, C. Stockmann, et al., Differential activation and antagonistic function of HIF-{alpha} isoforms in macrophages are essential for NO homeostasis, Genes Dev. 24 (5) (2010) 491–501, https://doi.org/10.1101/gad.1881410.

[45] A.E. Postlethwaite, L.J. Harris, S.H. Raza, S. Kodura, T. Akhigbe, Pharmacotherapy of systemic sclerosis, Expert Opin. Pharmacother. 11 (5) (2010) 789–806, https://doi.org/10.1517/14656561003592177.

[46] P.E. Lazzerini, M. Natale, E. Gianchecchi, P.L. Capecchi, C. Montilli, S. Zimbone, et al., Adenosine A2A receptor activation stimulates collagen production in scleroderma dermal fibroblasts either directly and through a cross-talk with the cannabinoid system, J. Mol. Med. (Berl.) 90 (3) (2012) 331–342, https://doi.org/10.1007/s00109-011-0824-5.

[47] V. Katchan, P. David, Y. Shoenfeld, Cannabinoids and autoimmune diseases: a systematic review, Autoimmun. Rev. 15 (6) (2016) 513–528, https://doi.org/10.1016/j.autrev.2016.02.008.

[48] R.B. Zurier, S.H. Burstein, Cannabinoids, inflammation, and fibrosis, FASEB J 30 (11) (2016) 3682–3689, https://doi.org/10.1096/fj.201600646R.

[49] C. Del Rio, I. Cantarero, B. Palomares, M. Gomez-Canas, J. Fernandez-Ruiz, C. Pavicic, et al., VCE-004.3, a cannabidiol aminoquinone derivative, prevents bleomycin-induced skin fibrosis and inflammation through PPARgamma- and CB2 receptor-dependent pathways, Br. J. Pharmacol. 175 (19) (2018) 3813–3831, https://doi.org/10.1111/bph.14450.

[50] J.L. Sargent, Z. Li, A.O. Aliprantis, M. Greenblatt, R. Lemaire, M.H. Wu, et al., Identification of optimal mouse models of systemic sclerosis by interspecies comparative genomics, Arthritis Rheumatol. 68 (8) (2016) 2003–2015, https://doi.org/10.1002/art.39658.

[51] S.A. Pendergrass, R. Lemaire, I.P. Francis, J.M. Mahoney, R. Lafyatis, M.L. Whitfield, Intrinsic gene expression subsets of diffuse cutaneous systemic sclerosis are stable in serial skin biopsies, J. Invest. Dermatol. 132 (5) (2012) 1363–1373, https://doi.org/10.1038/jid.2011.472.

[52] A.T. Dantas, A.R. de Almeida, M. Sampaio, M.F. Cordeiro, L.F. da Rocha Jr., P.S.S. de Oliveira, et al., Corticosteroid inhibits chemokines production in systemic sclerosis patients, Steroids 127 (2017) 24–30, https://doi.org/10.1016/j.steroids.2017.08.012.

[53] A.J. Gilbane, C.P. Denton, A.M. Holmes, Scleroderma pathogenesis: a pivotal role for fibroblasts as effector cells, Arthritis Res. Ther. 15 (3) (2013) 215, https://doi.org/10.1186/ar4230.

[54] K.H. Hong, S.A. Yoo, S.S. Kang, J.J. Choi, W.U. Kim, C.S. Cho, Hypoxia induces expression of connective tissue growth factor in scleroderma skin fibroblasts, Clin. Exp. Immunol. 146 (2) (2006) 362–370, https://doi.org/10.1111/j.1365-2249.2006.03199.x.

[55] M. Wu, S. Assassi, The role of type 1 interferon in systemic sclerosis, Front. Immunol. 4 (2013) 266, https://doi.org/10.3389/fimmu.2013.00266.

[56] J.N. Fleming, R.A. Nash, W.M. Mahoney Jr., S.M. Schwartz, Is scleroderma a vasculopathy? Curr. Rheumatol. Rep. 11 (2) (2009) 103–110, https://doi.org/10.1007/s11926-009-0015-3.

[57] S. Indraccolo, Interferon-alpha as angiogenesis inhibitor: learning from tumor models, Autoimmunity 43 (3) (2010) 244–247, https://doi.org/10.3109/08916930903510963.

[58] G. Beatty, Y. Paterson, IFN-gamma-dependent inhibition of tumor angiogenesis by tumor-infiltrating CD4+ T cells requires tumor responsiveness to IFN-gamma, J. Immunol. 166 (4) (2001) 2276–2282, https://doi.org/10.4049/jimmunol.166.4.2276.

[59] E. Romano, M. Manetti, I. Rosa, B.S. Fioretto, L. Ibba-Manneschi, M. Matucci-Cerinic, et al., Slit2/Robo4 axis may contribute to endothelial cell dysfunction and angiogenesis disturbance in systemic sclerosis, Ann. Rheum. Dis. 77 (11) (2018) 1665–1674, https://doi.org/10.1136/annrheumdis-2018-213239.

[60] M. Yang, M. Guo, Y. Hu, Y. Jiang, Scube regulates synovial angiogenesis-related signaling, Med. Hypotheses 81 (5) (2013) 948–953, https://doi.org/10.1016/j.mehy.2013.09.001.

[61] A.E. Abdulle, G.F.H. Diercks, M. Feelisch, D.J. Mulder, H. van Goor, The role of oxidative stress in the development of systemic sclerosis related vasculopathy, Front. Physiol. 9 (2018) 1177, https://doi.org/10.3389/fphys.2018.01177.

[62] S.A. Jimenez, Role of endothelial to mesenchymal transition in the pathogenesis of the vascular alterations in systemic sclerosis, ISRN Rheumatol. 2013 (2013) 835948, , https://doi.org/10.1155/2013/835948.

[63] A. Palazon, A.W. Goldrath, V. Nizet, R.S. Johnson, HIF transcription factors, inflammation, and immunity, Immunity 41 (4) (2014) 518–528, https://doi.org/10.1016/j.immuni.2014.09.008.

[64] S.A. Cotton, A.L. Herrick, M.I. Jayson, A.J. Freemont, Endothelial expression of nitric oxide synthases and nitrotyrosine in systemic sclerosis skin, J. Pathol. 189 (2) (1999) 273–278, https://doi.org/10.1002/(SICI)1096-9896(199910)189:2<273::AID-PATH413>3.0.CO;2-4.

[65] D.I. Gabrilovich, S. Nagaraj, Myeloid-derived suppressor cells as regulators of the immune system, Nat. Rev. Immunol. 9 (3) (2009) 162–174, https://doi.org/10.1038/nri2506.

[66] J.T. Pesce, T.R. Ramalingam, M.M. Mentink-Kane, M.S. Wilson, K.C. El Kasmi, A.M. Smith, et al., Arginase-1-expressing macrophages suppress Th2 cytokine-driven inflammation and fibrosis, PLoS Pathog. 5 (4) (2009) e1000371, , https://doi.org/10.1371/journal.ppat.1000371.

[67] X. Sun, W. Altalhi, S.S. Nunes, Vascularization strategies of engineered tissues and their application in cardiac regeneration, Adv. Drug Deliv. Rev. 96 (2016) 183–194, https://doi.org/10.1016/j.addr.2015.06.001.

[68] M.M. Bekhite, A. Finkensieper, J. Rebhan, S. Huse, S. Schultze-Mosgau, H.R. Figulla, et al., Hypoxia, leptin, and vascular endothelial growth factor stimulate vascular endothelial cell differentiation of human adipose tissue-derived stem cells, Stem Cells Dev. 23 (4) (2014) 333–351, https://doi.org/10.1089/scd.2013.0268.

[69] A.R. Mackie, D.W. Losordo, CD34-positive stem cells: in the treatment of heart and vascular disease in human beings, Tex. Heart Inst. J. 38 (5) (2011) 474–485.

[70] A. Scheja, A. Akesson, P. Geborek, M. Wildt, C.B. Wollheim, F.A. Wollheim, et al., Von Willebrand factor propeptide as a marker of disease activity in systemic sclerosis (scleroderma), Arthritis Res. 3 (3) (2001) 178–182, https://doi.org/10.1186/ar295.

[71] M. Kuwana, Y. Okazaki, H. Yasuoka, Y. Kawakami, Y. Ikeda, Defective vasculogenesis in systemic sclerosis, Lancet 364 (9434) (2004) 603–610, https://doi.org/10.1016/S0140-6736(04)16853-0.

[72] J.D. Schumacher, G.L. Guo, Regulation of hepatic stellate cells and fibrogenesis by fibroblast growth factors, Biomed Res. Int. 2016 (2016) 8323747, https://doi.org/10.1155/2016/8323747.

[73] V. Jimenez, C. Jambrina, E. Casana, V. Sacristan, S. Munoz, S. Darriba, et al., FGF21 gene therapy as treatment for obesity and insulin resistance, EMBO Mol. Med. 10 (8) (2018), https://doi.org/10.15252/emmm.201708791.

[74] M.E. Pitulescu, I. Schmidt, B.D. Giaimo, T. Antoine, F. Berkenfeld, F. Ferrante, et al., Dll4 and Notch signalling couples sprouting angiogenesis and artery formation, Nat. Cell Biol. 19 (8) (2017) 915–927, https://doi.org/10.1038/ncb3555.

[75] S. Zhao, X. Xiao, S. Sun, D. Li, W. Wang, Y. Fu, et al., MicroRNA-30d/JAG1 axis modulates pulmonary fibrosis through Notch signaling pathway, Pathol. Res. Pract. 214 (9) (2018) 1315–1323, https://doi.org/10.1016/j.prp.2018.02.014.

[76] G.S. Bogatkevich, A. Ludwicka-Bradley, K.B. Highland, F. Hant, P.J. Nietert, C.B. Singleton, et al., Down-regulation of collagen and connective tissue growth factor expression with hepatocyte growth factor in lung fibroblasts from white scleroderma patients via two signaling pathways, Arthritis Rheumatism 56 (10) (2007) 3468–3477, https://doi.org/10.1002/art.22874.

[77] C. Inampudi, E. Akintoye, T. Ando, A. Briasoulis, Angiogenesis in peripheral arterial disease, Curr. Opin. Pharmacol. 39 (2018) 60–67, https://doi.org/10.1016/j.coph.2018.02.011.